



1 **Evaluating impacts of climate change on future water scarcity in an**  
2 **intensively managed semi-arid region using a coupled model of biophysical**  
3 **processes and water rights**

4

5 **Bangshuai Han<sup>1\*</sup>, Shawn G. Benner<sup>2,3</sup>, and Alejandro N. Flores<sup>2,3\*</sup>**

6 <sup>1</sup>*Natural Resources and Environmental Management, Ball State University, Muncie, IN, 47304*

7 <sup>2</sup>*Geosciences, Boise State University, Boise, ID, 83725, USA*

8 <sup>3</sup>*Human-Environment Systems, Boise State University, Boise ID, 83725, USA*

9 *\*Corresponding authors: B. Han, [bhan@bsu.edu](mailto:bhan@bsu.edu); A.N. Flores, [lejoflores@boisestate.edu](mailto:lejoflores@boisestate.edu)*

10 **Key Points:**

- 11 • A new efficient method that captures the plausible range of variability of future  
12 climate change along with central tendencies
- 13 • A model that explicitly captures the spatiotemporally varying irrigation activities  
14 as constrained by local water rights
- 15 • An application to a semi-arid watershed to project water scarcity patterns under  
16 future climate change scenarios

17

18



## 19 **Abstract**

20 In semiarid and arid regions with intensively managed water supplies, water scarcity is a  
21 product of interactions between complex biophysical processes and human activities.  
22 Evaluating water scarcity under climate change necessitates modeling how these  
23 coupled processes interact and redistribute waters in the system under alternative  
24 climate conditions. A particular challenge on the climate input lies in adequately  
25 capturing the plausible range of variability of future climate change along with central  
26 tendencies. This study generates a large ensemble of daily climate realizations by  
27 combining a stochastic weather generator, historical climate observations, and  
28 statistically downscaled General Circulation Model projections. Three climate change  
29 scenario groups, reflecting the historical, RCP4.5, and RCP8.5 conditions, are  
30 developed. A modeling framework is built using the Envision alternative futures  
31 modeling platform to 1) explicitly capture the spatiotemporally varying irrigation activities  
32 as constrained by local water rights; and 2) project water scarcity patterns under climate  
33 change. The study area is the Treasure Valley, an irrigation-intensive semi-arid human-  
34 environment system. Climate projections for the region show future increases in both  
35 precipitation and temperature. The projected increase in temperature has a significant  
36 influence on the increase of the allocated and unsatisfied irrigation amount. Projected  
37 changes in precipitation produce more modest responses. The scenarios identify  
38 spatially distinct areas more sensitive to water scarcity, highlight the importance of  
39 climate change as a driver of scarcity, and identify potential shortcomings of the current  
40 water management. The approach of creating climate ensembles overcomes  
41 deficiencies of using a few or mean values of individual GCM realizations.



42 **Key words:**

43 Climate change, weather generator, general circulation models, water security, water  
44 rights, integration

45 **1. Introduction**

46 Simulations of the global climate system, often called General Circulation Models  
47 (GCMs), provide valuable insight into future climate change [Stocker et al., 2014]. There  
48 is a growing need to extend these climate model scenarios to regional and local water  
49 resources to understand potential impacts at a scale relevant to policy decision making  
50 (Giorgi et al., 2009). Climate change is anticipated to impact water resources in a  
51 variety of ways including increased vapor pressure deficits associated with higher  
52 temperatures [Will et al., 2013], increased frequency of extreme flooding and drought  
53 [Cai et al., 2014], shifts in precipitation phase from snow to rain, and changes in the  
54 timing and rate of melt of mountain snowpacks [Klos et al., 2014; Vano et al., 2015]. In  
55 arid and semi-arid systems where water availability is limited, e.g., the Western US,  
56 areas of the Iberian Peninsula, etc., climate change may stress the capacity of physical,  
57 cyber, and/or social infrastructure that has been developed to supply sufficient water to  
58 meet demands [Bosher et al., 2007; Marston and Cai, 2016].

59 Despite the importance of climate change on water resources, incorporating the effects  
60 of climate change into regional hydrologic model is challenging, as both climate and  
61 hydrologic systems are complex with numerous underlying uncertainties [Fowler et al.,  
62 2007]. Large-scale GCMs are most appropriately used for predicting climate change at



63 global scales, and large ensemble experiments with GCMs have shown significant  
64 regional, decadal-scale variability despite strong agreement at the global scale  
65 [Dominguez et al., 2012; Fildes and Kourentzes, 2011]. Statistical and dynamical  
66 downscaling methods have been developed to take outputs from GCMs and create  
67 forcings for models in an effort to assess climate change impacts at regional and local  
68 scales. However, and despite the increasingly sophisticated process representations  
69 within GCMs and improved spatial resolution, GCMs are not designed for the  
70 application of hydrological responses to climate change, and little confidence can be  
71 placed in application at daily time scales [Ashfaq et. al., 2010; Wilby and Wigley, 1997].

72 Due to internal climate variability, single realizations from climate models are often  
73 insufficient for model comparison to the observational record, model intercomparison,  
74 and future projections [Kay et al., 2015]. For example, research has found that even  
75 models sharing similar parameterization schemes may produce considerably different  
76 daily precipitation statistics [Frei et al., 2003]. Slight changes of the initialization of a  
77 GCM have been shown to produce completely different regional climate realizations  
78 after decades due to the internal randomness and chaos, even though the models still  
79 produce consensus estimates at the global scales [Kay et al., 2015]. This climate  
80 internal variability/uncertainty can be transferred and enlarged in the daily hydrological  
81 models when simulating hydrological runoff responses [Chen et al., 2012].

82 To overcome this, previous studies have been using multiple downscaled GCMs to  
83 incorporate a range of climate change projections [Abatzoglou and Brown, 2012], or  
84 using the averaged values from multiple GCMs to reduce the uncertainties from



85 individual GCMs [Fordham and W., 2011]. Currently available dynamically and  
86 statistically downscaled datasets used for climate change impacts studies at regional  
87 scales do not adequately capture uncertainties both within and between climate models  
88 in a way that can support robust quantification of the probability distribution function of  
89 outcomes of interest, like insufficiencies in water supply.

90 What is needed are large ensembles of realizations of forcings to drive regional models  
91 that capture uncertainties within individual GCMs, as well as variability across GCMs.  
92 Developing forcing ensembles using either statistical and/or dynamical downscaling  
93 [Abatzoglou and Brown, 2012; Dosio and Paruolo, 2011] can be prohibitively expensive  
94 because of requirements of storage, computational time, or both. Nevertheless,  
95 projections of future climate derived from GCMs reflect our best current knowledge of  
96 future climatic conditions and judicious and thoughtful use in regional climate impacts  
97 and adaptation studies remains a promising path forward. It is important to recognize, in  
98 particular, that no single climate model reliably represents future climate at the  
99 spatiotemporal scales required to support regional and local climate change impacts  
100 assessments.

101 Stochastic weather generators represent a potentially useful tool to help overcome  
102 some of the challenges of downscaling of GCMs. Stochastic weather generators [Chen,  
103 et al., 2010; Richardson, 1981; Richardson and Wright, 1984; Semenov and  
104 Barrow, 1997; Wilks, 2010] were developed to create plausible realizations of weather  
105 variables (particularly temperature, precipitation, and other environmental variables) at  
106 locations and temporal resolutions when only climatic statistics are available. Typically,



107 stochastic weather generators take as input climatic parameters like the average  
108 duration of time between storms, average storm duration and depth, monthly average  
109 daytime high temperature and produce realizations of variables like precipitation  
110 intensity, air temperature, and wind speed at temporal resolutions of days or hours. In  
111 generating realizations of weather variables, they often rely on a number of simplifying  
112 assumptions (e.g., exponential distribution of between-storm duration, etc.). They have  
113 the advantage of being far more computationally efficient than, for example, using a  
114 numerical weather model to generate weather conditions at a location. As a result,  
115 stochastic weather generators are useful for generating large ensembles of weather  
116 conditions required as input to models.

117 At the same time, stochastic weather generators are associated with important  
118 limitations with the assumptions underlying the form of the weather generator itself and,  
119 perhaps more importantly, the stationarity of the climate processes summarized by the  
120 statistics required as input. Specifically, stochastic weather generators cannot predict  
121 future climate change because they assume stationarity in the underlying statistics  
122 provided as input. Moreover, care is required when using stochastic weather generators  
123 to create environmental model forcings to evaluate sensitivities to future climate change  
124 because the climate statistics input to stochastic weather generators are likely  
125 correlated and cannot be perturbed independently of each other. Additionally, due to the  
126 intrinsic uncertainties associated with the output of stochastic weather generators (i.e.,  
127 the output of a weather generator is a single realization of a stochastic process) it is not  
128 possible to identify a single realization as being the most representative or useful. To  
129 robustly characterize the probabilistic behavior environmental systems in response to



130 uncertain forcings it is necessary to: (1) generate an ensemble of realizations of  
131 weather, (2) use this ensemble to create a corresponding ensemble of environmental  
132 outcomes by supplying each weather realization as input to an environmental model,  
133 and (3) examine the central tendency and variability across all outcomes.

134 In this work, we develop a framework for combining the outputs of statistically  
135 downscaled output from multiple GCMs with stochastic weather generators to evaluate  
136 the probabilistic potential impacts of climate change on a coupled socio-hydrologic  
137 system. Using the combination of GCM output and stochastic weather generators has  
138 previously been used to examine hydrological and ecological impacts of climate change  
139 [Mikhail, 1997; Xu, 1999]. These previous studies, however, relied on output from only  
140 one GCM projection, thereby missing potential impacts of climate change across  
141 uncertainties associated with the spectrum of GCMs currently used for global climate  
142 change analysis as part of the Intergovernmental Panel on Climate Change (IPCC)  
143 quadrennial review. In this study, we extend previous efforts by developing techniques  
144 to use information from multiple GCMs along with an existing stochastic weather  
145 generator to produce a suite of daily weather variables useful for a broad range of  
146 environmental models. The developed method first uses statistically downscaled output  
147 from multiple GCMs to derive an empirical probability distribution function of key  
148 statistics required as input to the stochastic weather generator. Then the method uses a  
149 statistic weather generator (WXGN) to create an ensemble of realizations of weather  
150 and applies it to a hydrologic model.



151 We use this approach to examine the potential ramifications of climate change in a  
152 coupled socio-hydrological system through an integrated hydrologic model in an  
153 irrigation-intensive, semi-arid watershed. In particular, the coupled socio-hydrological  
154 model simulates both biophysical hydrological processes, as well as redistribution of  
155 water in accordance with the spatiotemporal regime of water rights operating in the  
156 region. By creating an ensemble of climate impacts, this approach allows us to project  
157 both future water use and scarcity under three climate change scenarios. An outcome of  
158 particular value is insight into the spatial and temporal distribution of disruptions to water  
159 supply predicted by the simulations. This information may be at a spatiotemporal scale  
160 that is of direct value to stakeholders to help manage their limited water resources.  
161 What follows is a description of the methodological approach and experimental setup, a  
162 summary of relevant results, and a discussion of potential implications, limitations, and  
163 extensions of this work.

## 164 **2. Methods**

### 165 **2.1 Using downscaled GCMs to drive stochastic weather generator**

#### 166 **2.1.1 The WXGN weather generator**

167 A stochastic weather generator produces synthetic time series of weather data of  
168 specified length for a location based on statistical characteristics of observed weather at  
169 that location [Bouzaher et al., 1994]. Due to its consistency and simplicity, various  
170 stochastic weather generators have been designed, built, tested and applied [Chen et  
171 al., 2010; Flecher et al., 2010; Forsythe et al., 2014; Hayhoe and Stewart, 1996; Ivanov,





172 2007; Kilsby et al., 2007; Qian et al., 2004; Racsco, 1991; Richardson, 1981;  
173 Richardson and Wright, 1984; Semenov and Barrow, 1997; Wilks, 2010]. WXGN  
174 (varyingly also abbreviated as WGEN or WXGEN in the literature) is a frequently used  
175 weather generator for daily weather variables that are used in various hydrologic,  
176 agricultural, or environmental models, specifically being developed to support the  
177 Environmental Policy Integrated Climate (EPIC) Model, Agricultural  
178 Policy/Environmental eXtender (APEX) Model, and Soil & Water Assessment Tool  
179 (SWAT). WXGN is based on the daily weather data generator developed by Richardson  
180 [1981] and Richardson & Wright [1984]. While many stochastic weather generators only  
181 focus on “major” weather variables such as rainfall and/or temperature, WXGN  
182 generates a comprehensive package of daily weather parameters for any number of  
183 years for a location. Generated variables include precipitation, maximum and minimum  
184 temperature, relative humidity, solar radiation, wind speed, and wind direction. It is  
185 designed to preserve the dependence in time, internal correlation, and the seasonal  
186 characteristics that exist in actual weather and climate data [Richardson and Wright,  
187 1984]. In WXGN, precipitation and wind are generated independent of other variables.  
188 Precipitation is simulated using a first-order Markovian technique that produces time  
189 series of daily occurrence of precipitation (i.e., wet or dry days). On wet days,  
190 precipitation amount is generated using a skewed normal distribution. Maximum  
191 temperature, minimum temperature, and solar radiation are generated based on a  
192 continuous multivariate stochastic process, and constrained by whether the day is wet  
193 or dry [Richardson, 1981]. Relative humidity is obtained from a triangular distribution  
194 that takes into account the occurrence of rainfall on a particular day. Wind speed is



195 generated using a two-parameter gamma distribution that with location and shape  
196 parameters related to the velocity and frequency of the velocity. Wind direction is  
197 simulated using an empirical frequency distribution of wind direction specific for each  
198 location which is essentially the cumulative probability distribution from the monthly  
199 percentages of wind from each of the 16 directions given by the “Climate Atlas of the  
200 United States”. To estimate wind direction for any day, WXGN draws a uniformly  
201 distributed random number and locates its position on the appropriate monthly  
202 cumulative probability distribution of the wind direction.

### 203 **2.1.2 Climate change scenarios design**

204 Three broad climate categories are developed using the stochastic weather generator to  
205 facilitate the assessment of climate change effects on water resources. These  
206 categories include:

207 1) Historical: This scenario group evaluates a 30-year historical period as a baseline,  
208 against which the two other categories of climate change impacts are compared.

209 2) RCP4.5: This scenario group adopts the GCM projections from IPCC Representative  
210 Concentration Pathways (RCPs) RCP4.5, reflecting the stabilization scenario in which  
211 total radiative forcing is assumed to be stabilized before 2100 by employing a range of  
212 technologies and strategies for reducing greenhouse gas emissions. It assumes that net  
213 anthropogenic radiative forcing values in the year 2100 will be 4.5 W/m<sup>2</sup> above  
214 preindustrial values.



215 3) RCP8.5: This scenario group adopts the GCM projections from IPCC RCP8.5,  
216 reflecting increasing greenhouse gas emissions over time. This scenario group  
217 represents the most extreme warming outlook captured by the IPCC assessment and is  
218 meant to represent a “business as usual” response to global warming. It represents a  
219 net anthropogenic radiative forcing of  $8.5 \text{ W/m}^2$  relative to preindustrial values in the  
220 year 2100.

221 For each scenario group, we generate an ensemble of realizations of daily weather  
222 variables required as input to a model of a coupled socio-hydrological system, using the  
223 WXGN stochastic weather generator. We explicitly represent uncertainty in future  
224 projections of climate change by sampling the climate parameters required as input to  
225 WXGN from an empirical distribution function representing multiple GCMs. We then use  
226 these daily weather ensembles to force an existing model of a coupled socio-  
227 hydrological system based on the Envision framework [Bolte et al., 2006]. We compare  
228 simulations of future climate against the benchmark historical simulations, allowing us to  
229 compare both the central tendencies of future changes to the system along with  
230 potential ranges of variability about those central tendencies. Details are provided  
231 below.

### 232 **Figure 1 The flow chart of climate data generation**

233 Daily climate data were extracted from weather stations (historical) and downscaled  
234 GCMs (projections of RCP4.5 and RCP8.5). The data were then summarized to get  
235 monthly climate variables which were then statistically analyzed to get the  
236 representative ranges (25% to 75%). Future projections of the monthly climate variables



237 were generated using a Latin Hypercube Sampling. Then Ensembles of daily variables  
238 were generated using statistical weather generator (WXGN). These data (210 sets of  
239 30-yr daily climate data) were then employed as input for Envision runs to drive the  
240 integrated hydrologic model.

## 241 **2.2 Climate data collection and processing**

242 The flowchart of climate data collection and processing is shown in Figure 1. The  
243 historical climate data corresponds to observations collected at the Boise Air Terminal  
244 weather station from 1980 – 2014. Future regional climate projections were adopted  
245 from MACAv2-METDATA dataset, which used the Multivariate Adaptive Constructed  
246 Analogs (MACA) statistical downscaling method to downscale GCMs from the Coupled  
247 Model Inter-Comparison Project 5 (CMIP5) [Abatzoglou and Brown, 2012]. The dataset  
248 has been bias corrected and was trained using the gridded, high resolution (4 km), daily  
249 surface meteorological dataset METDATA [Abatzoglou, 2013], which was bias  
250 corrected and validated against an extensive network of weather stations including  
251 RAWS, AgriMet, AgWeatherNet, and USHCN-2. A total of 20 GCMs were downscaled,  
252 and 11 downscaled GCMs were selected due to the data availability at the time of  
253 downloading, and data completeness (Table 1). The data are then processed following  
254 the steps below.

### 255 **Table 1 CMIP5 models used in this study for downscaled climate data and the** 256 **model development centers**

#### 257 **Step #1: Analyzing representative ranges**



258 13 climate variables ( $V_i$ ) that are needed by WXGN for the generation of daily weather  
259 files are calculated and summarized for the historical observations and downscaled  
260 GCMs of RCP4.5 and RCP8.5 (Table 2). This step creates one set of climate variable  
261 statistics for the historical climate, and 11 sets of climate variable statistics for the 11  
262 sets of GCMs. Each set of climate variable statistics include average monthly climate  
263 variables as shown in Table 2. The historical scenario group only has one set of climate  
264 variable statistics. However, for the RCP4.5 and RCP8.5 scenario groups, multiple  
265 GCMs incorporate extreme values that are “outliers” of general future climate  
266 projections in the variable statistics (Figure 2). As such, we used the 25<sup>th</sup> and 75<sup>th</sup>  
267 percentiles of each monthly variable statistics as the representative ranges of possible  
268 climate projections. For RCP4.5 and RCP8.5 scenario groups, we sorted the values of  
269 each variable statistics, and calculated the percentiles as  
270  $100 \times (0.5/n)th, 100 \times (1.5/n)th, \dots, 100 \times ([n-0.5]/n)th$  ( $n = 11$  in this case). Then the 25<sup>th</sup>  
271 percentile  $V_{i_{25th}}$  and the 75<sup>th</sup> percentile  $V_{i_{75th}}$  are linearly interpolated based on the closest  
272 percentile values, and we use the range between  $V_{i_{25th}}$  and  $V_{i_{75th}}$  to denote the  
273 representative values of the sample. This design removes the extreme variations of  
274 each variable statistics, and can better reflect the climate change paths that are more  
275 likely to occur by the projection of GCMs.

276 **Table 2: 13 climate variables summarized from GCMs for WXGN use to generate**  
277 **ensemble of daily climate realizations.**

278 **Figure 2: Boxplot of monthly climate variables over 11 GCMs, using only**  
279 **precipitation as an example. Boxplot of the other 12 variables is included in the**



280 **appendix A. The circles indicate the historical monthly precipitation. The large**  
281 **variance indicates that an ensemble of climate realizations is necessary to**  
282 **capture the variations of future climate change.**

### 283 **Step #2: Random sampling**

284 Latin Hypercube Sampling (LHS) was used to sample 10 sets of monthly climate  
285 statistics within the representative range ( $V_{i_{25th}} \sim V_{i_{75th}}$ ) of each variable statistics for  
286 RCP4.5 and RCP8.5 scenario groups. For a function of a certain number of variables,  
287 the LHS approach equally divides the range of each variable into M (here, M = 10)  
288 probable intervals. Within each interval, the variable is randomly sampled once. This  
289 method ensures that each variable is evenly sampled, and the M (here, M = 10) random  
290 sampled values for each variable will include values that have a relatively low probability  
291 of occurrence. As such, the approach allows a stable output with a much smaller  
292 number of samples than a simple Monte Carlo sampling. Since distributed daily  
293 hydrologic models are usually computationally expensive, this sampling method makes  
294 simulation more practical with limited number of samples. This step generates 10 sets  
295 of randomly sampled monthly statistics for RCP4.5 and RCP8.5 scenario groups,  
296 respectively.

### 297 **Step #3: Daily weather generation**

298 We used WXGN to create 10 sets of daily weather data based on each randomly  
299 sampled RCP4.5 and RCP8.5 variable statistics, and the historical monthly statistics.  
300 This step creates 100 sets of 30-year (3000 years) future daily weather data for the



301 RCP4.5 scenario group, 100 sets of 30-yr (3000 years) of future daily weather data for  
302 the RCP8.5 scenario group, and 10 sets of 30-yr (300 years) of future daily weather  
303 data for the historical scenario group. The daily data reflects the statistics of the 10 sets  
304 of samples from RCP4.5, 10 sets of samples from RCP8.5, and the 1 set of statistics  
305 from historical observations. These daily weather datasets, reflecting future climate  
306 scenarios, were then served as inputs for the daily time step hydrologic model in  
307 Envision.

### 308 **2.3 Coupled socio-hydrology systems model**

309 An integrated socio-hydrologic model that simulates spatially explicit water use based  
310 on local water rights is used to evaluate spatiotemporal patterns of water scarcity in the  
311 context of potential future climate. A detailed overview of the biophysical and water  
312 rights components of the model, the datasets used to parameterize boundary  
313 conditions, calibration to and verification against historical data, and limitations of the  
314 model in the context of those calibration/verification exercises was previously described  
315 by Han et al. [2017]. Here we provide a brief overview of the key model components  
316 pertinent to this study.

317 The socio-hydrologic model is developed within the Envision modeling framework, a  
318 spatially explicit multi-agent simulation platform for evaluating potential landscape  
319 changes arising from interactions between and among complex biophysical and social  
320 processes [Bolte et al., 2006]. The model used here employs a slightly revised semi-  
321 conceptual Hydrologiska Byråns Vattenbalansavdelning (HBV) model to simulate  
322 hydrologic processes. The HBV model is implemented here as a semi-lumped model,



323 operating on spatial elements of Hydrologic Response Units (HRUs) with relatively  
324 similar elevation and land cover. At each HRU, the instantaneous temporal change in  
325 five water reservoirs (snow, soil moisture, an upper groundwater reservoir, a lower  
326 groundwater reservoir, and lake storage) is balanced by incoming precipitation,  
327 outgoing evapotranspiration, and outgoing runoff fluxes. Precipitation phase (snow vs.  
328 rain) is determined based on whether the daily average air temperature exceeds a  
329 constant threshold. Evapotranspiration is modeled using the FAO56 Penman–Monteith  
330 method as specified by the UN Food and Agriculture Organization (FAO) in paper  
331 number 56 (Allen et al., 1998) and in Allen and Robison (2007). In this approach,  
332 potential evapotranspiration at each HRU is the product of a land use dependent crop  
333 coefficient and a calculated reference potential evapotranspiration corresponding to full-  
334 cover alfalfa, given the meteorological forcings of that day. Runoff is parameterized  
335 through a series of three outflow equations wherein runoff is linearly proportional to  
336 water in excess of a threshold value in the upper groundwater reservoir, storage in the  
337 upper groundwater reservoir, and storage lower groundwater reservoir. The constants  
338 of proportionality for these outflow equations are treated as calibrated parameters.  
339 Runoff generated at each HRU is routed via two quasi-linear equations to the stream  
340 network (represented by hydrography data), wherein channel routing is treated as a  
341 linear reservoir process.

342 Irrigation activities are simulated based on water rights data provided by the Idaho  
343 Department of Water Resources; these water rights are based on the Doctrine of Prior  
344 Appropriation (Tarlock, 2000). Each record in the water rights dataset is associated  
345 with: 1) a priority date on which a water user is entitled to withdrawals from the surface





346 water distribution system, 2) the geographic point of diversion, 3) the maximum  
347 diversion rate from the point, and 4) the geographic place of use. Within each time step  
348 and for each HRU, the model examines the available water in the stream, the  
349 biophysical water demand of the agricultural land within the HRU, and the water rights  
350 associated with a place of use coincident with the HRU. Water allocated for irrigation is  
351 the minimum of these three quantities. The unsatisfied water is the difference between  
352 the amount of water demanded and allocated for each place of use in the model. The  
353 model was calibrated and validated by varying the parameters using a Monte-Carlo  
354 approach and comparing the simulated hydrographs with observations under historical  
355 conditions corresponding to water years 2006-2013. Detailed descriptions of the  
356 calibration and validation processes, and the underlying algorithms are described by  
357 Han et al., [2017].

358 As previously stated, the upstream surface water hydrology boundary condition in the  
359 Lower Boise River Basin corresponds to hydrologic output of a system of large  
360 reservoirs within the Upper Boise River Basin, a snow-dominated, mountain, largely  
361 forest covered, watershed. Although climate change, particularly in the form of shifts in  
362 precipitation phase from snow to rain, is expected to significantly alter hydrologic  
363 regimes in the Upper Boise River Basin, we do not consider these potential changes in  
364 order to reduce the complexity of our analysis. As such, the upstream inflow boundary  
365 to our simulation domain (the discharge from the Lucky Peak Reservoir) is set to be the  
366 same as a normal year, taking 2012 as an example. While future changes in water  
367 rights depend on future real estate transactions, growth in the extent of urban areas,  
368 and potential changes in water rights laws, we assume that the attributes of the water



369 rights data remain the same over time. Further, we do not take into account  
370 technological changes that may significantly increase water use efficiency in the  
371 agricultural sector and lead to a lower irrigation water demand and actual water use in  
372 the future. Given these assumptions, the impacts of climate change on water availability  
373 at the watershed were quantified based on the allocated irrigation amount and the  
374 unsatisfied irrigation amount for the years from 2071 to 2100. Since the weather  
375 generator replicates overall statistics instead of “predicting” inter-annual differences, the  
376 comparison between any specific two years within a scenario group are meaningless.  
377 As such, we treat the data of each year as an independent realization of the potential  
378 outcomes within the large ensemble of data over the thirty years of simulation.  
379 Ensemble characteristics and statistics are then compared between the three scenario  
380 groups.

#### 381 **2.4 Datasets used in the model**

382 Environmental forcing data used in this study corresponds to statistically downscaled  
383 output from a suite of GCMs that are summarized in Table 1. Each forcing dataset  
384 includes daily precipitation, maximum temperature, minimum temperature, specific  
385 humidity, solar radiation, and wind speed. These variables, required as input drivers to  
386 the socio-hydrologic model, were extracted for the grid point that coincides with the  
387 Boise Air Terminal (43.5644° N, 116.2228° W) for the years 2071-2100 to represent the  
388 local future climate. Historical data of the same forcing variables at Boise Air Terminal  
389 were obtained from the National Climatic Data Center and National Solar Radiation  
390 Database for the period 1981-2014. Water rights data was obtained from the Idaho



391 Department of Water Resources, which provides the point of diversion, priority date,  
392 maximum allowable allocation, and place of use records required as input to the socio-  
393 hydrologic model, updated as of 2010. We selected only those records associated with  
394 an irrigation water use. Input to the Boise River at the upstream boundary of the domain  
395 corresponds to daily historical discharge from Lucky Peak reservoir for calendar year  
396 2012, and is assumed consistent between years and were obtained from the US Bureau  
397 of Reclamation Pacific Northwest Hydromet database. Land use data corresponds to  
398 the National Landcover Dataset (NLCD 2011) and is used to both to construct the  
399 computational domains and HRUs and in calculation of evapotranspiration. Stream and  
400 watershed boundaries were obtained from the NHDPlus Version 2 dataset, which  
401 provides geospatial data used in flow routing. These datasets are summarized in Table  
402 3.

## 403 **2.5 Study area**

404 The study site corresponds to the Lower Boise River Basin, also known as the Treasure  
405 Valley, in southwest Idaho, USA (Figure 3). The region is the most populous and rapidly  
406 growing area within the state and serves as a natural laboratory for studying ongoing  
407 challenges associated with population growth, urbanization, agricultural production, and  
408 climate and hydrologic change. Climate in the Treasure Valley is generally consistent  
409 with a semi-arid Mediterranean with hot, dry summers and cold, wet winters. In the  
410 absence of agricultural and developed land uses, vegetation cover in the region is  
411 consistent with the Sagebrush-steppe ecosystem of the larger Great Basin ecoregion.  
412 Historical average precipitation is 296 mm/y at the Boise Air Terminal weather station.



413 Importantly, the Treasure Valley is home to Idaho's three largest cities (Boise, Meridian,  
414 and Nampa). Population of the Boise City-Nampa Metropolitan Statistical Area (MSA)  
415 was estimated to be 690,423 as of 2016, up from 616,561 in the 2010 Census, an  
416 average annual increase of 1.9%. Thus, the Treasure Valley region is being subjected  
417 to significant land use conversion, resulting in changes to biophysical and social  
418 systems, and interactions between the two.

419 Climate exerts a significant control on the use of water resources within the region.  
420 More than half of the total precipitation that falls within the Treasure Valley, which is not  
421 sufficient to support many high-value crops, occurs during the non-irrigation season. As  
422 such, local agriculture relies heavily on irrigation water from the Upper Boise River  
423 Basin, particularly during the hot, dry portion of the growing season. Climate change  
424 driven increase in temperatures in the Treasure Valley not only increases atmospheric  
425 water demand during the growing season, but impacts of climate change shifts the  
426 timing, amount, and phase of precipitation that will lead to earlier runoff and increased  
427 variability from the Upper Boise River Basin.

428 Irrigation is facilitated by a series of reservoirs upstream of the Treasure Valley that  
429 store and regulate water from the Upper Boise River Basin. Lucky Peak Reservoir,  
430 which is operated jointly by the US Army Corps of Engineers and the Bureau of  
431 Reclamation for purposes of flood control and irrigation water supply, is the lower-most  
432 of these reservoirs. Water released from Lucky Peak Reservoir flows along the Boise  
433 River for about 103 km (64 miles) northwestward through the Treasure Valley to its  
434 confluence with the Snake River. A number of canals and diversion dams have been  
435 built along the Boise River to divert water to water rights holders, the vast majority of



436 which are farmers using the water for irrigation. Irrigation has dramatically altered the  
437 originally desert landscape into a patchwork of seasonally irrigated agricultural lands of  
438 varying crops. Urban growth, shifts in crops grown in the Treasure Valley associated  
439 with global market demands, and changes in irrigation practices (e.g., shifts from  
440 flooding to sprinkler and drip irrigation) drive changes in the spatial patterns of land and  
441 water use. Despite the importance of water resources and potential threats of water  
442 scarcity, there have been limited studies regarding future water availability and scarcity  
443 in this region [Petrich, 2004; Urban and Petrich, 1996]. This research aims to examine  
444 the agricultural irrigation water demand and water scarcity under future climate change  
445 scenarios, using the generated ensemble of climate change realizations. The work is  
446 built upon an integrated hydrologic model that incorporates hydrological processes and  
447 the irrigation activities which follow the local water rights. Three important outcomes of  
448 this study are 1) a methodology that facilitates the creation of an ensemble of climate  
449 change scenarios that is suitable for daily hydrologic model input; 2) A modeling  
450 framework for the integration of hydrological processes, human irrigation activities, and  
451 climate change; 3) References to help local stakeholders with decision making to adapt  
452 to future climate change.

453 **Figure 3: Study area: the Treasure Valley.**

### 454 **3. Results**

#### 455 **3.1 Climate change analysis**

456 To illustrate the degree to which the use of the stochastic weather generator captures  
457 variation in key climate parameters across GCMs, we show the probability density



458 functions (PDFs) of the output of the stochastic weather generator for annual  
459 precipitation amount, maximum temperature and minimum temperature (Figure 4).  
460 Overall, the most likely precipitation amount in the RCP8.5 scenario group is larger than  
461 that in the RCP4.5 group and Historical group, as shown in the probability density  
462 function figure (Figure 4). The average annual precipitation increases by 11% from  
463 Historical to RCP4.5 conditions, and by 29% to RCP8.5 conditions. However, a  
464 significant overlap between precipitation probability density functions exist in the three  
465 scenario groups. For example, it is likely that precipitation in RCP8.5 is smaller than that  
466 in RCP4.5 or even Historical group in some sets of climate realizations.

467 The PDFs of maximum temperature and minimum annual temperature increase  
468 significantly in the future, and are much narrower in comparison to the precipitation  
469 pattern (Figure 5). The annual mean maximum/minimum temperature is highest in the  
470 RCP8.5 scenario group, lowest in the Historical scenario group. The maximum  
471 temperature in RCP8.5 group is consistently higher, on average by 4.1 °C than the  
472 temperature in the Historical group. The maximum temperature in the RCP4.5 group is  
473 consistently larger than that in the Historical group by an average of 1.7 °C. The  
474 minimum temperature in RCP8.5 is consistently larger than that in the Historical  
475 scenario by an average of 5.6 °C. The minimum temperature in RCP4.5 is consistently  
476 larger than that in the Historical group by an average of 3.2 °C. The average daily  
477 temperature increases by 4.9 °C in RCP8.5 scenario group, and by 2.5 °C in the  
478 RCP4.5 scenario group. Temperature increase in the Treasure Valley is at the higher  
479 end of the IPCC CIMP5 projected global trend which, in general, projects a temperature



480 increase of 1.1°C to 2.6°C for RCP4.5, and an increase of 2.6°C to 4.8°C for RCP8.5 by  
481 the end of the 21<sup>st</sup> century [T F Stocker, 2014].

482 **Figure 4: The annual precipitation used to drive the hydrologic model**

483 **Figure 5: The annual maximum (Tmax) and minimum (Tmin) temperatures used to**  
484 **drive the hydrologic model**

### 485 3.3 Irrigation water analysis

486 The simulation results from a total of 210 runs of the integrated socio-hydrologic model  
487 indicate, unsurprisingly, that more irrigation water is needed to fulfill the crop water  
488 demand in the future. The average annual allocated irrigation water is highest in the  
489 RCP8.5 scenario group (Figure 6). The average annual allocated irrigation water in both  
490 RCP4.5 ( $8.2 \times 10^5$  acre-feet) and RCP8.5 ( $8.9 \times 10^5$  acre-feet) scenario groups is higher  
491 than the Historical scenario ( $6.7 \times 10^5$  acre-feet), an increase of 22% and 33%,  
492 respectively. However, the ensemble between the three scenarios overlap one another  
493 due to the extremes captured by realizations of the weather generator. This overlap  
494 indicates extreme water use scenarios that deviate significantly from the average future  
495 projections. As such, although examining the mean/median values from a large  
496 ensemble of analysis is useful for understanding the central tendencies of potential  
497 future agricultural water demands in the region, the entirety of the ensemble allows a  
498 more sophisticated interpretation of potential future outcomes, particularly those that  
499 could be low probability events but of significant consequences.



500 **Figure 6: The annual amount of allocated irrigation water under 3 different**

501 **scenarios**

502 Similar to the allocated amount, the average annual unsatisfied irrigation water is also  
503 highest for RCP8.5 scenario group (Figure 7). The average annual unsatisfied irrigation  
504 water in both RCP4.5 and RCP8.5 scenario groups are higher than the Historical  
505 scenario group. Similar with allocated irrigation water, there is also overlap in  
506 unsatisfied irrigation between all scenarios. The mean value of the unsatisfied water  
507 increases from about  $1.7 \times 10^4$  acre-feet in the Historical scenario group to about  $2.7 \times$   
508  $10^4$  acre-feet in the RCP4.5 scenario group and  $4.2 \times 10^4$  acre-feet in the RCP8.5  
509 scenario group, an increase of 59% and 147%, respectively. The results underscore the  
510 value of using ensembles of model simulations to assess potential future outcomes, as  
511 a few realizations were associated with extreme values of unsatisfied irrigation that are  
512 not reflected the central tendencies of the PDFs.

513 **Figure 7: The annual amount of unsatisfied irrigation water under 3 different**

514 **scenarios**

515 The ensemble simulation also allows us to assess spatial locations within the domain  
516 most likely to be associated with unsatisfied water demand under future climates and, by  
517 comparing to geospatial data characterizing biophysical and social constraints on  
518 hydrology in the region, to draw inference about key characteristics of the landscape  
519 associated with water shortages (Figure 8, Figure 9). The model-simulated allocation rate  
520 indicates that the southwest part of the study domain receives the most allocated water,  
521 while the corridor immediately abutting the downstream portions of the Boise River





522 receives relatively less allocated water. Conversely, the unsatisfied irrigation water is  
523 largest along the downstream Boise River.

524 However, there is also a significant amount of water scarcity in the southwest part of the  
525 domain (Wilder Irrigation District approximate to Lake Lowell). Throughout the domain,  
526 where there is water allocated to irrigation there is a significant increase in both water use  
527 and water scarcity relative to Historical conditions, in the RCP 4.5 and RCP 8.5 conditions.  
528 Looking more specifically at the southwest part (Wilder Irrigation District), the mean  
529 allocated irrigation rate increases from 737 mm/y to 909 mm/yr to 996 mm/yr from the  
530 Historical to the RCP4.5, and then to the RCP8.5 scenario groups, an increase of 23%  
531 and 35% respectively. Although the area is senior in water rights (water rights in the region  
532 were claimed between 1864 to 1927), the mean unsatisfied irrigation rate increases from  
533 13 mm/y to 19 mm/y to 31 mm/y from the Historical to the RCP 4.5, and then to the RCP  
534 8.5 scenario groups, an increase of 46% and 138% respectively. Using ensemble mean  
535 values avoids the large discrepancies from individual simulations. For example, the  
536 allocated irrigation rate at the 85 percentile varies from 789 mm/y in the Historical to 948  
537 mm/y in the RCP4.5 to 1041 mm/y in the the RCP8.5 groups, and the unsatisfied irrigation  
538 rate at the 85 percentile varies from 20 mm/y in the Historical to 27 mm/yr in the RCP4.5  
539 to 42 mm/yr in the RCP8.5 groups.

540 Figure 8: The annual amount of allocated irrigation water under 3 different scenario  
541 groups (Spatial Maps. Show mean, and 85 and 15 percent range for each scenario  
542 group)



543 Figure 9: The annual amount of unsatisfied irrigation water under 3 different scenario  
544 groups (Spatial Maps. Show mean, and 85 and 15 percent range for each scenario  
545 group)

#### 546 4. Discussion

##### 547 4.1 Adopting stochastic weather generators with GCM output

548 The use of multiple GCM projections in combination with the stochastic weather  
549 generator to generate ensembles of future climate realizations offers some key  
550 advantages in assessing the potential future ramifications for coupled socio-hydrologic  
551 systems. The results are broadly consistent with the GCM output, but also account  
552 for variability in climatic conditions as captured by a variety of GCMs while providing  
553 insights into local climatic perturbations

554 First, the method allows an unlimited number of future daily climate data with monthly  
555 statistics that are derived from multiple GCMs. In this way, the method avoids the  
556 deficiencies of using a single GCM or a simple mean of multiple GCMs that may lead to  
557 biased future projections, and avoids the deficiencies of limited number of GCMs that  
558 cannot provide enough reliable daily climate data for hydrologic models.

559

560 Second, stochastic weather generators (like WXGN) are a relatively computationally  
561 inexpensive method for generating daily climate variables needed by a diverse array of  
562 hydrologic and ecological models. They are also relatively easy to use and  
563 parameterize, making them amenable to a variety of different climate change



564 assessment applications and techniques. The resulting ensemble of outputs generated  
565 with the corresponding ensemble of climate realizations used as input allow for a more  
566 sophisticated analysis of potential future impacts of climate change, both in terms of the  
567 central tendencies of change and potentially low-risk, high-consequence outcomes.

568 It should be added that the proposed method is not appropriate for all circumstances.  
569 The method we develop and apply here is most suitable for hydrologic and ecologic  
570 models that needs numerous sets of long-term daily climate inputs. For example, in our  
571 case study, we need daily hydrologic simulation to allow for real-time water rights  
572 allocations. The method may not be necessary for all conceptual modes or lump-sum  
573 models that only require rough water balance estimations.

574 Although the application of the stochastic weather generator to create ensembles of  
575 climate input to a socio-hydrologic model is methodologically straightforward, simulating  
576 an ensemble of climate realizations still requires a relatively large amount of  
577 computational time. This is particularly true for spatially distributed hydrologic models.  
578 There is, therefore, a need to balance larger ensembles against higher spatial  
579 resolutions when a spatially distributed model is being used.

#### 580 **4.2 The effects of climate change on regional scale hydrology and irrigation**

581 Both temperature and precipitation are important climate variables that affect regional  
582 hydrology and irrigation demand. Temperature directly influences potential  
583 evapotranspiration and crop water demand (Figure 10, Figure 11). Under the same  
584 upstream inflow conditions, the allocated and unsatisfied irrigation water has a clear



585 monotonic relationship with temperature across scenario groups. There is an increase  
586 of allocated irrigation amount with the increase of maximum temperature and minimum  
587 temperature. Although there is significant overlap between scenario groups, the overall  
588 trend of an increasing irrigation water demand and scarcity from historical conditions to  
589 RCP4.5 and RCP8.5 is evident.

590 The influence of precipitation on allocated and unsatisfied water is not as clear as that  
591 of temperature (Figure 12). In the Treasure Valley, over half of the precipitation happens  
592 in the non-irrigation season, and most of the irrigation water relies on diversion from  
593 streams and reservoirs. As such, precipitation change in the immediate region of the  
594 Treasure Valley is not as important as temperature change with regard to water demand  
595 and use. Instead, precipitation in the upper Boise River Basin that provides snowpack  
596 for irrigation water will exert a more significant influence on downstream water demand.

597 **Figure 10 The scatterplot of the allocation irrigation amount and the unsatisfied**  
598 **irrigation amount with maximum and minimum temperature under three scenario**  
599 **groups. The solid dots indicate the mean values of each scenario group.**

600 **Figure 11 The annual amount of evapotranspiration rate under 3 different**  
601 **scenario groups**

602 **Figure 12 The scatterplot of the allocation irrigation amount and the unsatisfied**  
603 **irrigation amount with precipitation under three scenario groups. The solid dots**  
604 **indicate the mean values of each scenario group.**

#### 605 **4.3 Future work**

606 In illustrating the influence of climate change on the future water availability this work,  
607 does not consider population and land use change. Both of these factors will have



608 potentially significant influence on future water use in the region. Incorporating these  
609 potential land use changes would provide additional insight into changes to future water  
610 resources of the region. The present work also assumes that the input to the river  
611 system from the Upper Boise River Basin is captured by the observed flows in a typical  
612 year (calendar year 2012) in the Boise River. Despite these acknowledged limitations,  
613 this work illustrates the use of an ensemble-based method for climate change impact  
614 analysis that is of value in quantifying the central tendencies and variability about  
615 changes in future water use in a strongly coupled socio-hydrologic system.

## 616 **5. Conclusions**

617 This study develops an ensemble approach for creating daily climate realizations  
618 combining a stochastic weather generator and downscaled General Circulation Model  
619 (GCM) projections. The generated ensemble of climate data is then used to drive an  
620 integrated socio-hydrologic model using the Envision scenario-based modeling  
621 framework. In this way, the model captures both spatially explicit irrigation activities  
622 constrained by local water rights, and future changes in climate and their impact on  
623 atmospheric water demand in the region. We tested this model in a rapidly growing  
624 region of Idaho, USA. Results show that, on average, precipitation amount increases  
625 slightly and temperature increases significantly in future climate scenarios. Temperature  
626 increases are particularly pronounced in the RCP8.5 scenarios. The increase of  
627 temperature has direct influence on the increase of the allocated and unsatisfied  
628 irrigation amount, while the impacts of slightly increased mean annual precipitation (but  
629 increased interannual variability in mean annual precipitation) on water use are less



630 obvious and more uncertain. The model also predicts spatial patterns in water allocation  
631 and scarcity and the ensemble approach allows us to identify regions within the study  
632 area that will be more prone to insufficient water supply in the future. Although the  
633 developed model is associated with some key simplifications that limit, for instance, the  
634 ability to draw inferences about future groundwater-surface water interactions, the  
635 approach presented here could be applied to more sophisticated modeling frameworks  
636 to elicit broader conclusions about system behavior. Moreover, the framework  
637 presented here is portable to other geographic settings where legal frameworks dictate  
638 the timing, amount, and priority of water use.

639 **Author contributions:** Bangshuai Han and Alejandro N. Flores designed this research  
640 and interpreted the results. Bangshuai Han conducted the research. Bangshuai Han  
641 prepared the manuscript with the help with Shawn G. Benner, Alejandro N. Flores, and  
642 get agreement for submission with all co-authors.

#### 643 **ACKNOWLEDGMENTS**

644 This work was supported by grants from the National Science Foundation (NSF) Idaho  
645 Established Program to Stimulate Competitive Research (EPSCoR) under award number  
646 IIA-1301792, NSF CAREER Award EAR-1352631, and Ball State University new faculty  
647 start-up fund under award number 120198. We would like to thank Dr. Javier M. Osorio  
648 Leyton from Texas A&M for the help with WXGN, and Dr. Katherine Hegewisch from  
649 University of Idaho for the MACA data collection. We also thank the Envision team from  
650 Oregon State University for the help with the hydrologic model construction and



651 debugging. Data associated with this manuscript has been permanently archived and

652 made public with DOI: <https://doi.org/10.18122/B20133>.



653 **List of Tables**

654 *Table 1 CMIP5 models used in this study for downscaled climate data and the model*  
655 *development centers*

656 *Table 2 13 climate variables summarized from GCMs for WXGN use to generate*  
657 *ensemble of daily climate realizations*

658 *Table 3 Datasets used and the source link in the study*

659





660 **List of Figures**

- 661 *Figure 1 The flow chart of climate data generation. Daily climate data was extracted*  
662 *from weather stations (historical) and downscaled GCMs (projection of RCP4.5 and*  
663 *RCP8.5). The data were then summarized to get monthly climate variables which were*  
664 *then statistically analyzed to get the representative ranges (25% to 75%). Future*  
665 *projections of the monthly climate variables were generated using a Latin Hypercube*  
666 *Sampling. Then Ensembles of daily variables were generated using statistical weather*  
667 *generator (WXGN). These data (210 sets of 30-yr daily climate data) were then*  
668 *employed as input for Envision running to drive the integrated hydrologic model.*
- 669 *Figure 2: Boxplot of monthly climate variables over 11 selected GCMs, using only*  
670 *precipitation as an example. Boxplot of all variables are included in Appendix A. The*  
671 *circles indicate the historical monthly precipitation. The large variance indicates that an*  
672 *ensemble of climate realizations are necessary to capture the variations of future*  
673 *climate change. See Appendix A for boxplot of all monthly climate variables.*
- 674 *Figure 3 Study area: the Treasure Valley*
- 675 *Figure 4 The probability density function of the annual precipitation used to drive the*  
676 *hydrologic model.*
- 677 *Figure 5: The annual maximum (Tmax) and minimum (Tmin) temperatures used to drive*  
678 *the hydrologic model.*
- 679 *Figure 6 The annual amount of allocated irrigation water under 3 different scenario*  
680 *groups (Line figure. Show mean, and 85% and 15% range for each scenario group)*
- 681 *Figure 7 The annual amount of unsatisfied irrigation water under 3 different scenario*  
682 *groups*
- 683 *Figure 8 The annual amount of allocated irrigation water under 3 different scenario*  
684 *groups (Spatial Maps. Show mean, and 85 and 15 percent range for each scenario*  
685 *group)*
- 686 *Figure 9 The annual amount of unsatisfied irrigation water under 3 different scenario*  
687 *groups (Spatial Maps. Show mean, and 85 and 15 percent range for each scenario*  
688 *group)*
- 689 *Figure 10 The scatterplot of the allocation irrigation amount and the unsatisfied irrigation*  
690 *amount with maximum and minimum temperature under three scenario groups. The*  
691 *solid dots indicate the mean values of each scenario group.*
- 692 *Figure 11 The annual amount of evapotranspiration rate under 3 different scenario*  
693 *groups*
- 694 *Figure 12 The scatterplot of the allocation irrigation amount and the unsatisfied irrigation*  
695 *amount with precipitation under three scenario groups. The solid dots indicate the mean*  
696 *values of each scenario group.*
- 697  
698  
699



700

701 **Table 1 CMIP5 models used in this study for downscaled climate data and the**  
702 **model development centers**

Model	Development Center
<b>BNU-ESM</b>	College of Global Change and Earth System Science, Beijing Normal University, China
<b>CanESM2</b>	Canadian Center for Climate Modeling and Analysis
<b>CNRM-CM5</b>	National Center of Meteorological Research, France
<b>CSIRO-Mk3-6-0</b>	Commonwealth Scientific and Industrial Research Organization/Queensland Climate Change Center of Excellence, Australia
<b>GFDL-ESM2G</b>	NOAA Geophysical Fluid Dynamics Laboratory, USA
<b>GFDL-ESM2M</b>	NOAA Geophysical Fluid Dynamics Laboratory, USA
<b>IPSL-CM5A-LR</b>	Institut Pierre Smon Laplace, France
<b>IPSL-CM5A-MR</b>	Institut Pierre Smon Laplace, France
<b>IPSL-CM5B-LR</b>	Institut Pierre Smon Laplace, France
<b>MIROC5</b>	Atmosphere and Ocean Research Institute (The University of Tokyo), National Institute of Environmental Studies, and Japan Agency for Marine-Earth Science and Technology
<b>MRI-CGCM3</b>	Meteorological Research Institute, Japan

703

704



705 **Table 2 13 climate variables summarized from GCMs for WXGN use to generate**  
706 **ensemble of daily climate realizations**

<b>Variable</b>	<b>Description</b>
<b>PRECIP</b>	Average monthly precipitation
<b>TMAX</b>	Average monthly maximum air temperature
<b>TMIN</b>	Average monthly minimum air temperature
<b>PWD</b>	Monthly probability of wet day after dry day
<b>PWW</b>	Monthly probability of wet day after wet day
<b>DAYP</b>	Average number days of rain per month days
<b>RAD</b>	Average monthly solar radiation
<b>SDMX</b>	Monthly average standard deviation of daily maximum temperature
<b>SDMM</b>	Monthly average standard deviation of daily minimum temperature
<b>SDRF</b>	Monthly standard deviation of daily precipitation
<b>SKRF</b>	Monthly skew coefficient for daily precipitation
<b>RH</b>	Monthly average relative humidity (fraction)
<b>WS</b>	Average monthly wind speed

707

708



709 **Table 3 Datasets used and the source link in the study**

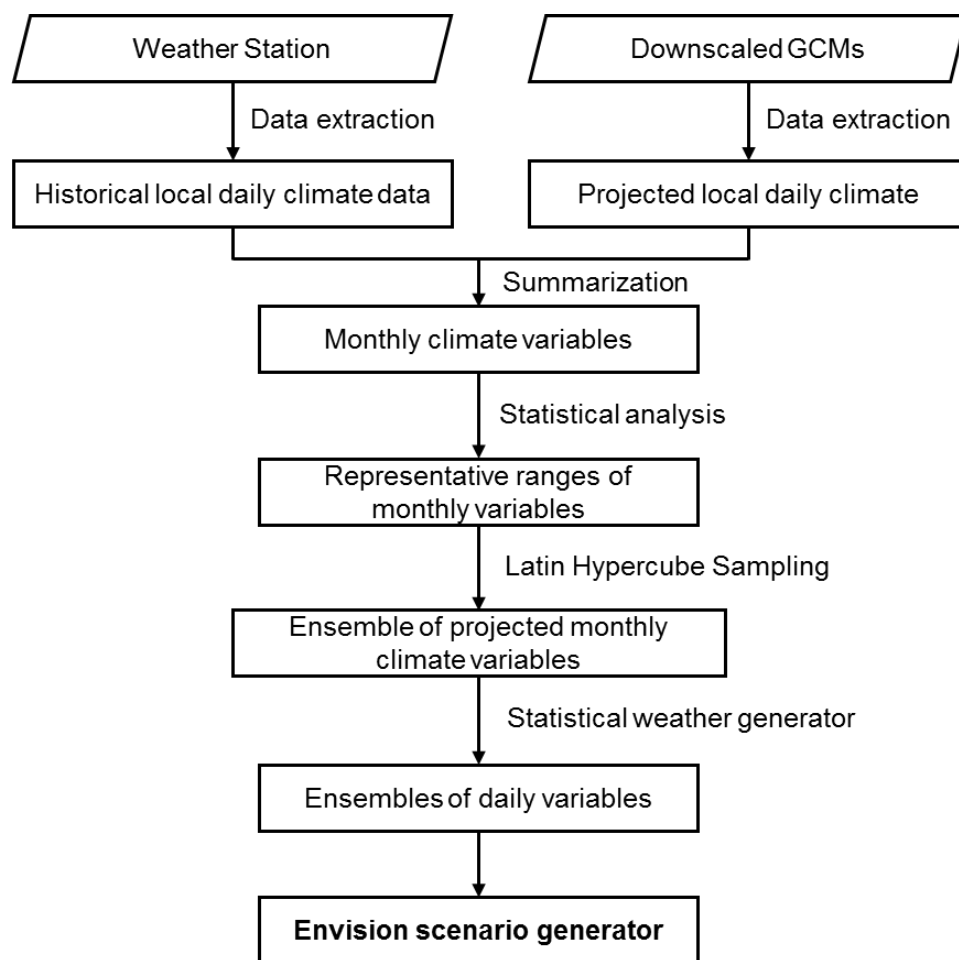
<b>Input Data</b>	<b>Data Source</b>	<b>Year</b>	<b>Use in Model</b>	<b>Link</b>
<b>Streams</b>	NHDPlus	2012	Build stream network and flow routing	<a href="http://www.horizon-systems.com/nhdplus/NHDPlusV2_17.php">http://www.horizon-systems.com/nhdplus/NHDPlusV2_17.php</a>
<b>Land use/land cover</b>	National Landcover dataset (NLCD)	2011	Evaportranspiration	<a href="http://www.mrlc.gov/nlcd2011.php">http://www.mrlc.gov/nlcd2011.php</a>
<b>Water Rights</b>	Idaho Department of Water Resources (IDWR)	2010	Irrigation (Watermaster)	<a href="http://www.idwr.idaho.gov/ftp/gisdata/Spatial/WaterRights">http://www.idwr.idaho.gov/ftp/gisdata/Spatial/WaterRights</a>
<b>Major climate variables</b>	National Climatic Data Center (NCDC)	1981-2014	Climate input	<a href="http://www7.ncdc.noaa.gov/CDO/cdodata.cmd">http://www7.ncdc.noaa.gov/CDO/cdodata.cmd</a>
<b>Solar radiation</b>	National Renewable Energy Laboratory (NREL)	1981-2010	Climate input	<a href="http://rredc.nrel.gov/solar/old_data/nsrdb/">http://rredc.nrel.gov/solar/old_data/nsrdb/</a>
<b>Reservoir Inflow</b>	Hydromet Pacific Northwest Region	2012	Inflow boundary	<a href="http://www.usbr.gov/pn/hydromet/arcread.html">http://www.usbr.gov/pn/hydromet/arcread.html</a>

710

711



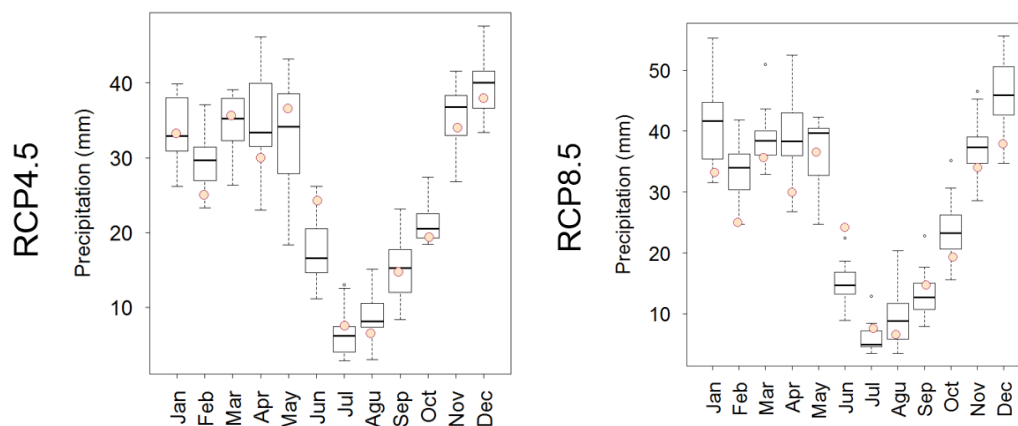
712



713

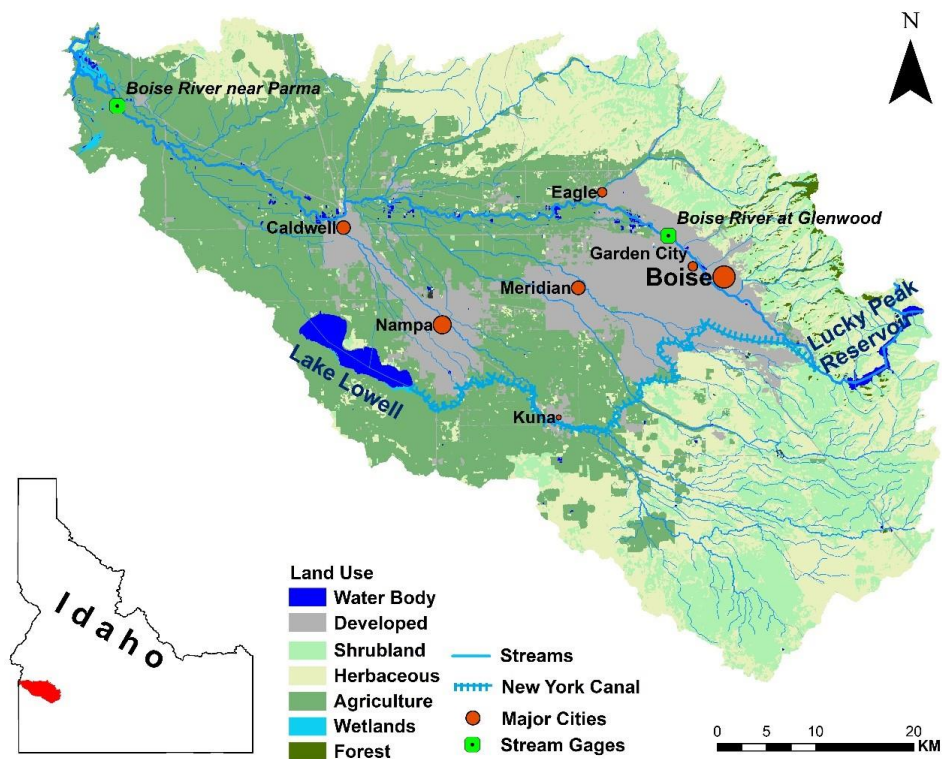
714 **Figure 1** The flow chart of climate data generation. Daily climate data was  
715 extracted from weather stations (historical) and downscaled GCMs (projection of  
716 RCP4.5 and RCP8.5). The data were then summarized to get monthly climate  
717 variables which were then statistically analyzed to get the representative ranges  
718 (25% to 75%). Future projections of the monthly climate variables were generated  
719 using a Latin Hypercube Sampling. Then Ensembles of daily variables were  
720 generated using statistical weather generator (WXGN). These data (210 sets of 30-  
721 yr daily climate data) were then employed as input for Envision running to drive  
722 the integrated hydrologic model.

723



724

725 **Figure 2** Boxplot of monthly climate variables over 11 selected GCMs, using only  
726 precipitation as an example. Boxplot of all variables are included in Appendix A.  
727 The circles indicate the historical monthly precipitation. The large variance  
728 indicates that an ensemble of climate realizations are necessary to capture the  
729 variations of future climate change. See Appendix A for boxplot of all monthly  
730 climate variables.

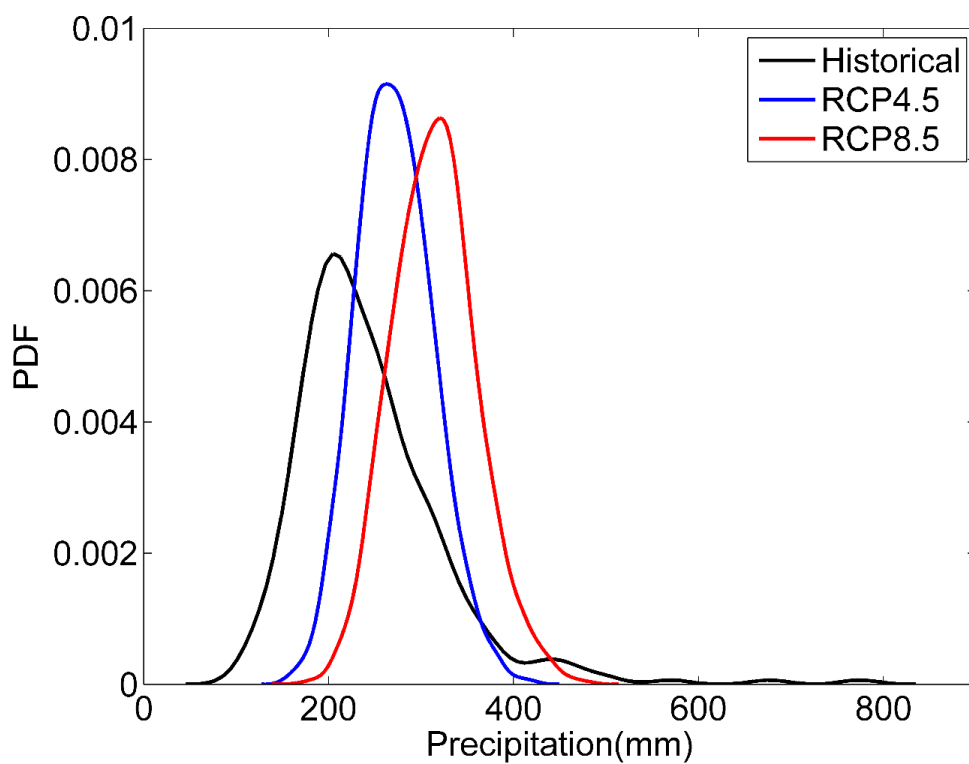


731

732 **Figure 3 Study area: the Treasure Valley**

733

734



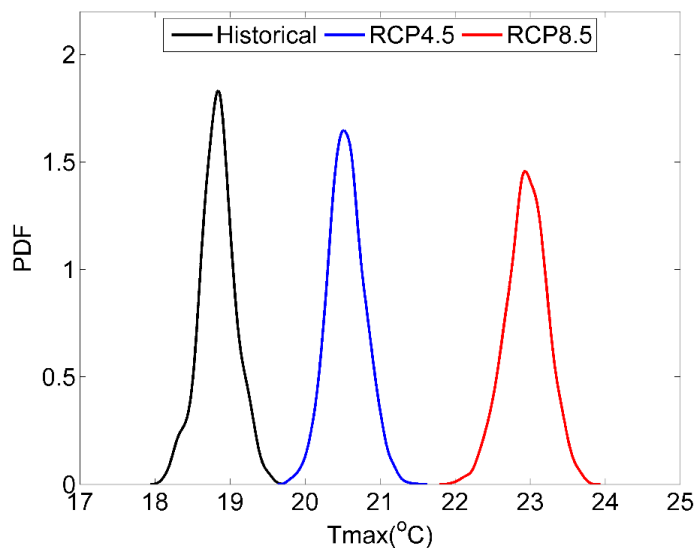
735

736

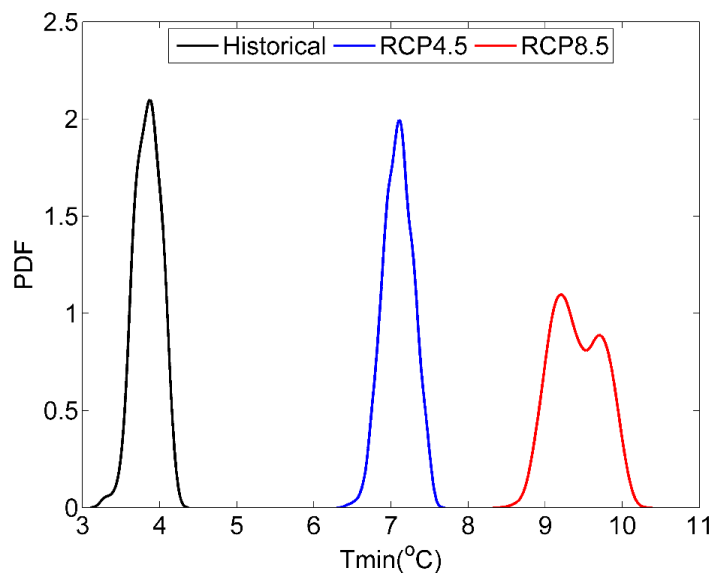
737

**Figure 4** The probability density function of the annual precipitation used to drive the hydrologic model.





738



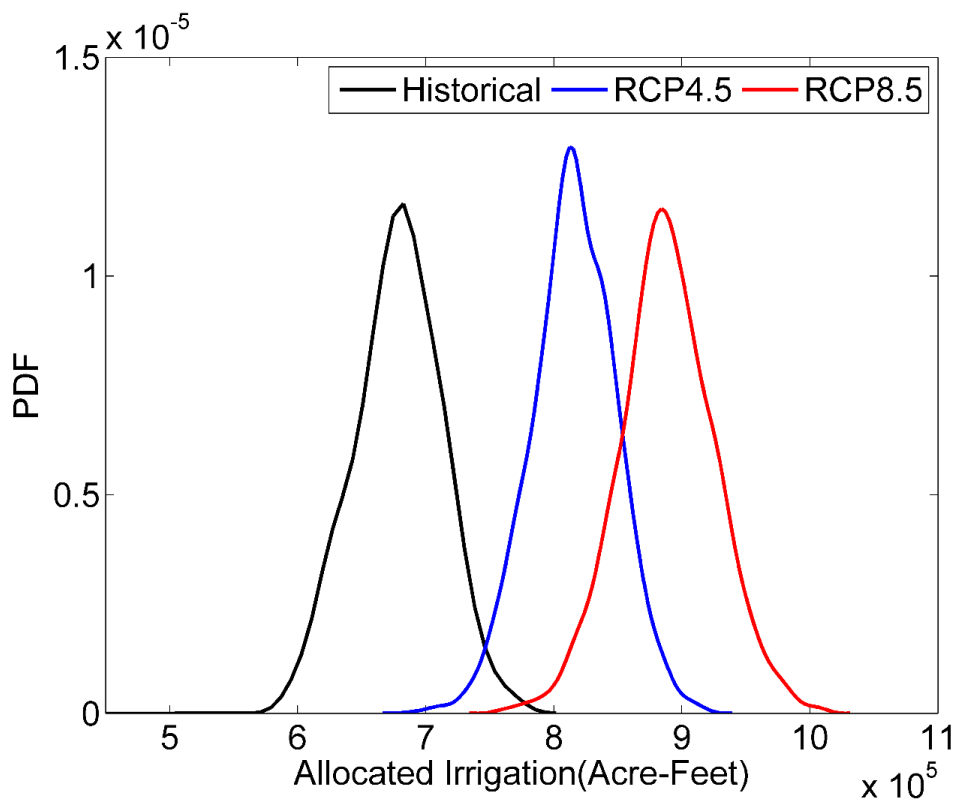
739

740

741 **Figure 5** The annual maximum (*Tmax*) and minimum (*Tmin*) temperatures used to  
742 drive the hydrologic model.  
743

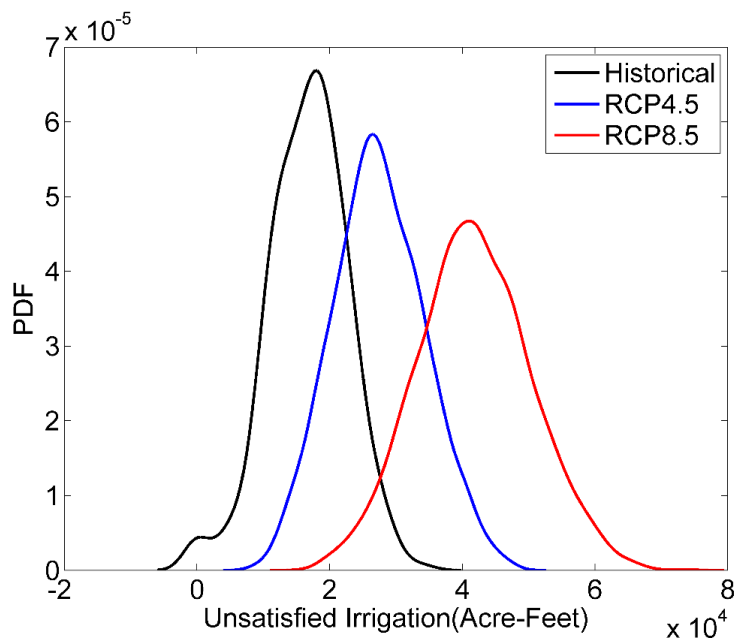
744

744



745  
746  
747  
748  
749  
750  
751

**Figure 6** The annual amount of allocated irrigation water under 3 different scenario groups (Line figure. Show mean, and 85% and 15% range for each scenario group)



752

753

754

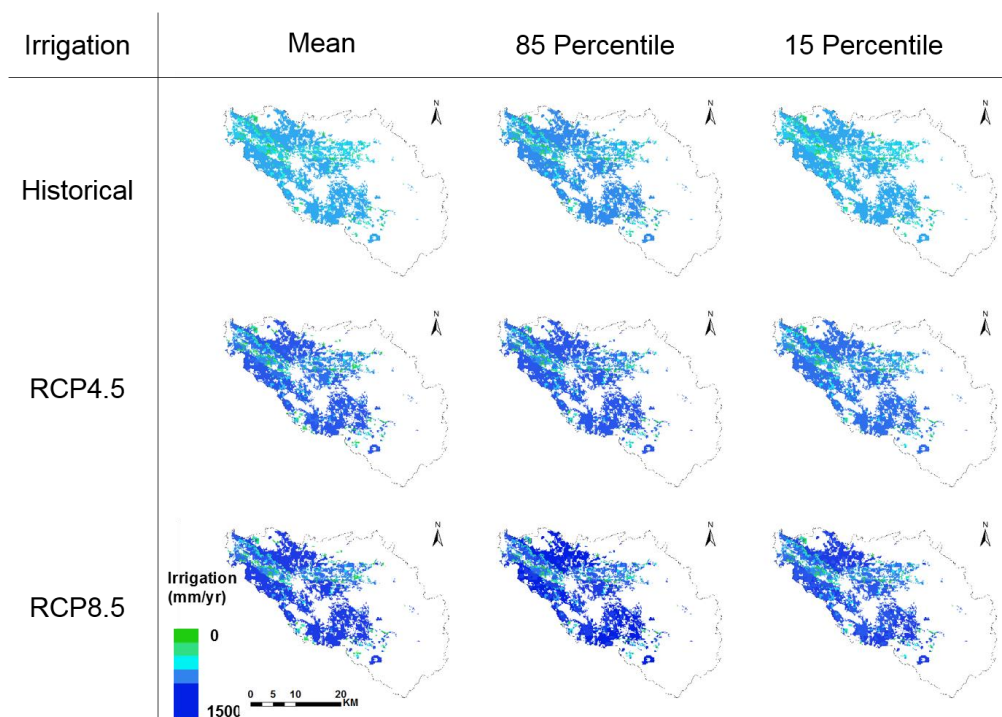
755

756

**Figure 7** The annual amount of unsatisfied irrigation water under 3 different scenario groups

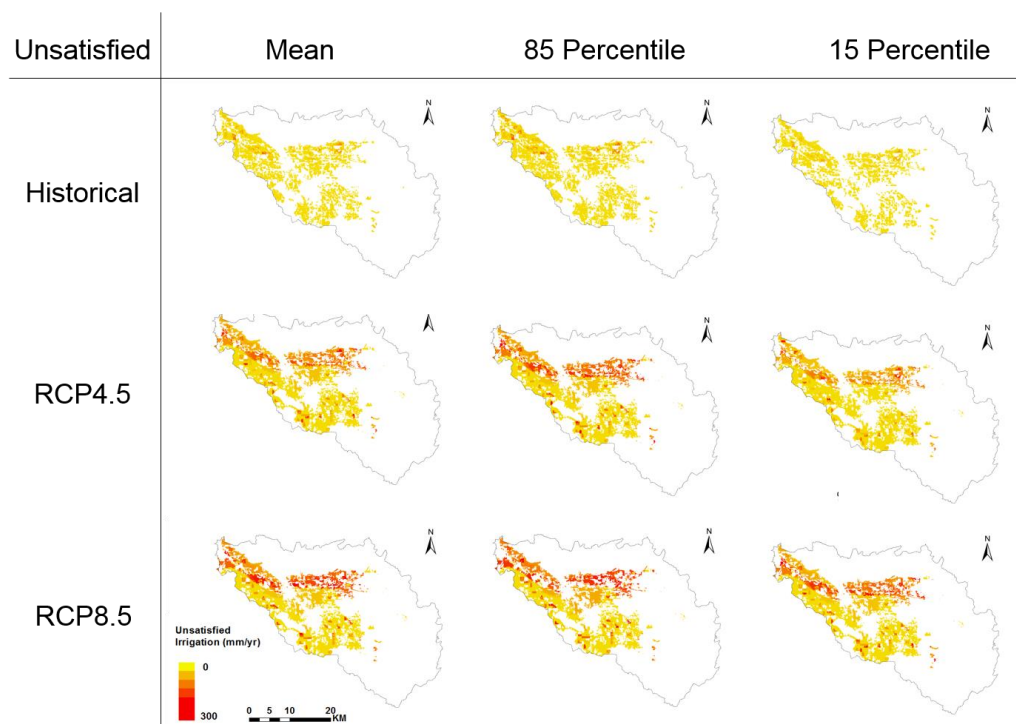


757



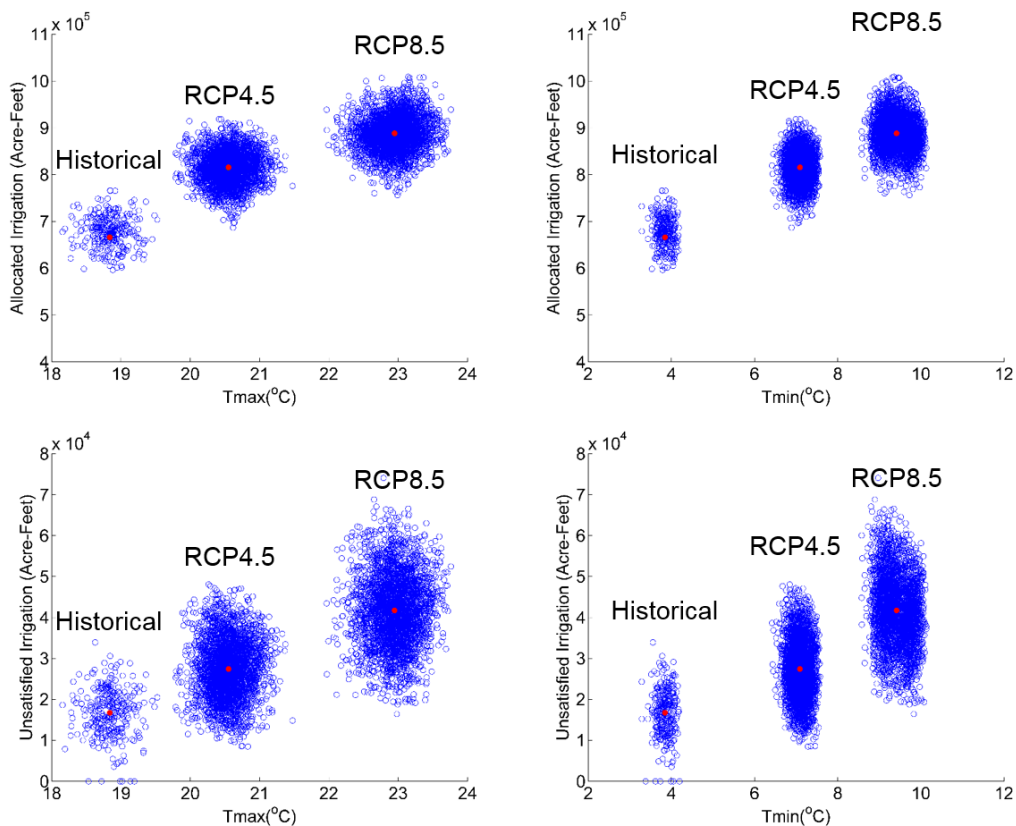
758

759 **Figure 8** The annual amount of allocated irrigation water under 3 different  
760 scenario groups (Spatial Maps. Show mean, and 85 and 15 percent range for each  
761 scenario group)



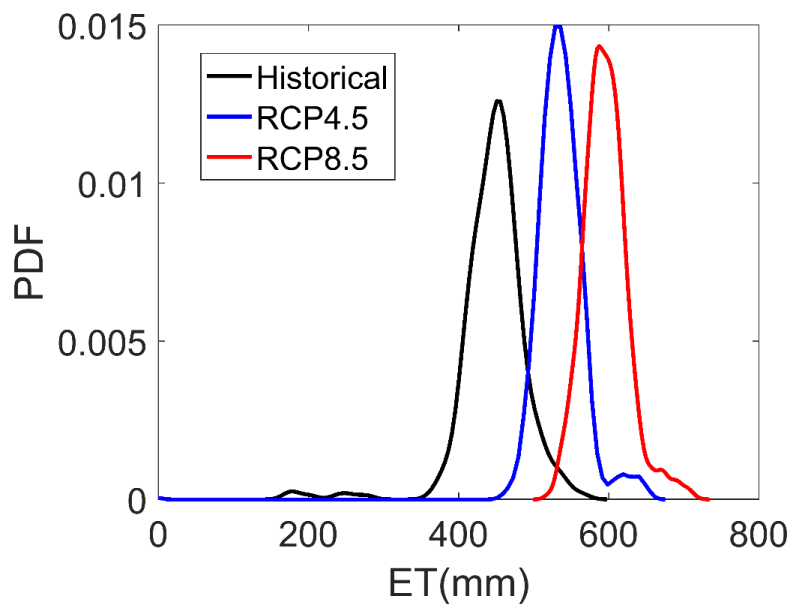
762

763 **Figure 9** The annual amount of unsatisfied irrigation water under 3 different  
 764 **scenario groups (Spatial Maps. Show mean, and 85 and 15 percent range for each**  
 765 **scenario group)**  
 766



767  
 768

769 **Figure 10** The scatterplot of the allocation irrigation amount and the unsatisfied  
 770 irrigation amount with maximum and minimum temperature under three scenario  
 771 groups. The solid dots indicate the mean values of each scenario group.  
 772



773

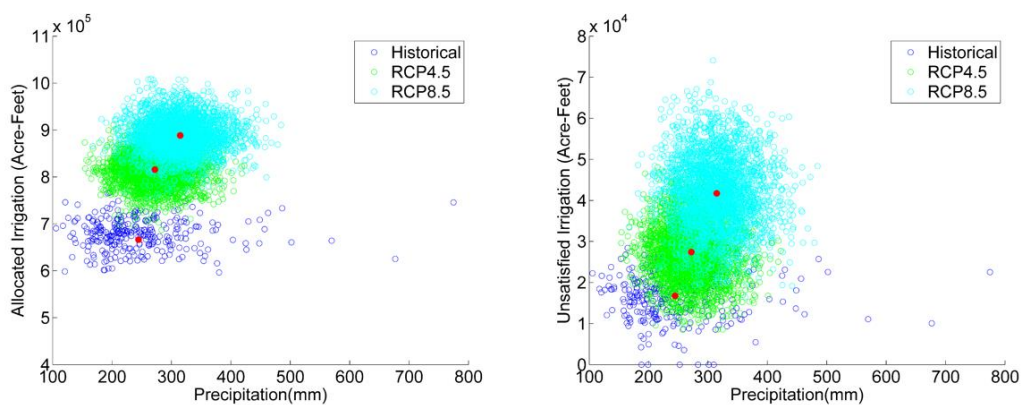
774 **Figure 11** *The annual amount of evapotranspiration rate under 3 different*  
775 *scenario groups*

776



777

778



779

780 **Figure 12 The scatterplot of the allocation irrigation amount and the unsatisfied**  
781 **irrigation amount with precipitation under three scenario groups. The solid dots**  
782 **indicate the mean values of each scenario group.**

783

784



785 **References:**

- 786 Abatzoglou, J. T., and T. J. Brown (2012), A comparison of statistical downscaling  
787 methods suited for wildfire applications, *International Journal of Climatology*,  
788 32(5), 772-780.
- 789 Abatzoglou, J. T. (2013). Development of gridded surface meteorological data for  
790 ecological applications and modelling. *International Journal of Climatology*, 33(1),  
791 121-131.
- 792 Ashfaq, M., L. C. Bowling, K. Cherkauer, J. S. Pal, and N. S. Diffenbaugh. "Influence of  
793 climate model biases and daily-scale temperature and precipitation events on  
794 hydrological impacts assessment: A case study of the United States." *Journal of*  
795 *Geophysical Research: Atmospheres (1984–2012)* 115, no. D14 (2010).
- 796 Bolte, J. P., D. W. Hulse, S. V. Gregory, and C. Smith (2006). Modeling biocomplexity–  
797 actors, landscapes and alternative futures. *Environmental Modelling &*  
798 *Software* 22, no. 5: 570-579.
- 799 Boshier, L., P. Carrillo, A. Dainty, J. Glass and A. Price (2007). Realising a resilient and  
800 sustainable built environment: towards a strategic agenda for the United  
801 Kingdom. *Disasters*, 31(3), pp.236-255.
- 802 Bouzaher, A., J. F. Shogren, D. Holtkamp, P. W. Gassman, D. Archer, P. G.  
803 Lakshminarayan, A. L. Carriquiry, and R. Reese (1994), *Agricultural Policies and*  
804 *Soil Degradation in Western Canada: An Agro-Ecological Economic Assessment*,  
805 *Report 2: The Environmental Modeling System*, Center for Agricultural and Rural  
806 *Development (CARD) at Iowa State University*.
- 807 Cai, W., S. Borlace, M. Lengaigne, P. Van Rensch, M. Collins, G. Vecchi, A.  
808 Timmermann, A. Santoso, M.J. McPhaden, L.Wu and M.H. England (2014).  
809 Increasing frequency of extreme El Niño events due to greenhouse  
810 warming. *Nature climate change*, 4(2), pp.111-116. doi:10.1038/nclimate2100.
- 811 Chen, H., X. Chong-Yu, and G. Shenglian (2012), Comparison and evaluation of  
812 multiple GCMs, statistical downscaling and hydrological models in the study of  
813 climate change impacts on runoff, *Journal of Hydrology*. Volumes 434–435, 36–  
814 45.
- 815 Chen, J., François P. B., and R. Leconte (2010). A daily stochastic weather generator  
816 for preserving low-frequency of climate variability. *Journal of hydrology* 388.3:  
817 480-490.
- 818 Dominguez, F., J. Cañon, and J. Valdes (2010), IPCC-AR4 climate simulations for the  
819 Southwestern US: the importance of future ENSO projections. *Climatic*  
820 *Change* 99, no. 3: 499-514. DOI: 10.1007/s10584-009-9672-5.
- 821 Dosio, A., and P. Paruolo (2011). Bias correction of the ENSEMBLES high-resolution  
822 climate change projections for use by impact models: evaluation on the present  
823 climate. *Journal of Geophysical Research: Atmospheres* 116.D16.
- 824 Fildes, R., and N. Kourentzes (2011). Validation and forecasting accuracy in models of  
825 climate change. *International Journal of Forecasting* 27, no. 4: 968-995.  
826 <https://doi.org/10.1016/j.ijforecast.2011.03.008>.
- 827 Flecher, C., P. Naveau, D. Allard, and N. Brisson (2010). A stochastic daily weather  
828 generator for skewed data. *Water Resources Research* 46, no. 7.



- 829 Fordham, D. A., Wigley, Tom M.L., and B. B. W. (2011), Multi - model climate  
830 projections for biodiversity risk assessments, *Ecological Applications*, 21(8),  
831 3317-3331.
- 832 Forsythe, N., H. J. Fowler, S. Blenkinsop, A. Burton, C. G. Kilsby, D. R. Archer, C.  
833 Harpham, and M. Z. Hashmi (2014), Application of a stochastic weather  
834 generator to assess climate change impacts in a semi-arid climate: The Upper  
835 Indus Basin, *Journal of Hydrology*, 517, 1019-1034.
- 836 Fowler, H. J., S. Blenkinsop, and C. Tebaldi (2007), Linking climate change modelling to  
837 impacts studies: recent advances in downscaling techniques for hydrological  
838 modelling, *International journal of climatology*, 27(12), 1547-1578.
- 839 Frei, C., J. H. Christensen, M. Déqué, D. Jacob, R. G. Jones, and P. L. Vidale (2003),  
840 Daily precipitation statistics in regional climate models: Evaluation and  
841 intercomparison for the European Alps, *Journal of Geophysical Research:*  
842 *Atmospheres*, 108(D3).
- 843 Giorgi, F., C. Jones and G.R. Asrar. (2009). Addressing climate information needs at  
844 the regional level: the CORDEX framework. World Meteorological Organization  
845 (WMO) Bulletin, 58(3), p.175.
- 846 Han, B., Benner, S. G., Bolte, J. P., Vache, K. B., and Flores, A. N. (2017). Coupling  
847 biophysical processes and water rights to simulate spatially distributed water use  
848 in an intensively managed hydrologic system, *Hydrol. Earth Syst. Sci.*, 21, 3671-  
849 3685, <https://doi.org/10.5194/hess-21-3671-2017>.
- 850 Hansen, J., M. Sato, and R. Ruedy (2012), Perception of climate change. *Proceedings*  
851 *of the National Academy of Sciences* 109.37: E2415-E2423.
- 852 Hayhoe, H. N., and D. W. Stewart (1996), Evaluation of CLIGEN and WXGEN weather  
853 data generators under Canadian conditions, *Canadian Water Resources Journal*,  
854 21(1), 53-67.
- 855 Ivanov, V. Y., R. L. Bras, and D. C. Curtis (2007). A weather generator for hydrological,  
856 ecological, and agricultural applications. *Water resources research* 43.10.
- 857 Kay, J. E., C. Deser, A. Phillips, A. Mai, C. Hannay, G. Strand, J. M. Arblaster, S. C.  
858 Bates, G. Danabasoglu, and J. Edwards (2015), The Community Earth System  
859 Model (CESM) large ensemble project: A community resource for studying  
860 climate change in the presence of internal climate variability, *Bulletin of the*  
861 *American Meteorological Society*, 96(8), 1333-1349.
- 862 Kilsby, C. G., P. D. Jones, A. Burton, A. C. Ford, H. J. Fowler, C. Harpham, P. James,  
863 A. Smith, and R. L. Wilby (2007), A daily weather generator for use in climate  
864 change studies, *Environmental Modelling & Software*, 22(12), 1705-1719.
- 865 Klos, P.Z., T.E. Link, and J.T. Abatzoglou (2014). Extent of the rain-snow transition  
866 zone in the western US under historic and projected climate. *Geophysical*  
867 *Research Letters*, 41(13), pp.4560-4568. DOI: 10.1002/2014GL060500.
- 868 Marston, L. and X. Cai (2016). An overview of water reallocation and the barriers to its  
869 implementation. *Wiley Interdisciplinary Reviews: Water*, 3(5), pp.658-677.
- 870 Mikhail A. Semenov, E. M. B. (1997), Use Of A Stochastic Weather Generator In The  
871 Development Of Climate Ch, *Climate Change*, 35(4), 397-414.
- 872 P. Racsco, L. S. (1991), A serial approach to local stochastic weather models, edited.  
873 Petrich, C. R. (2004), *Treasure Valley hydrologic project executive summary*, Idaho  
874 Water Resources Research Institute.

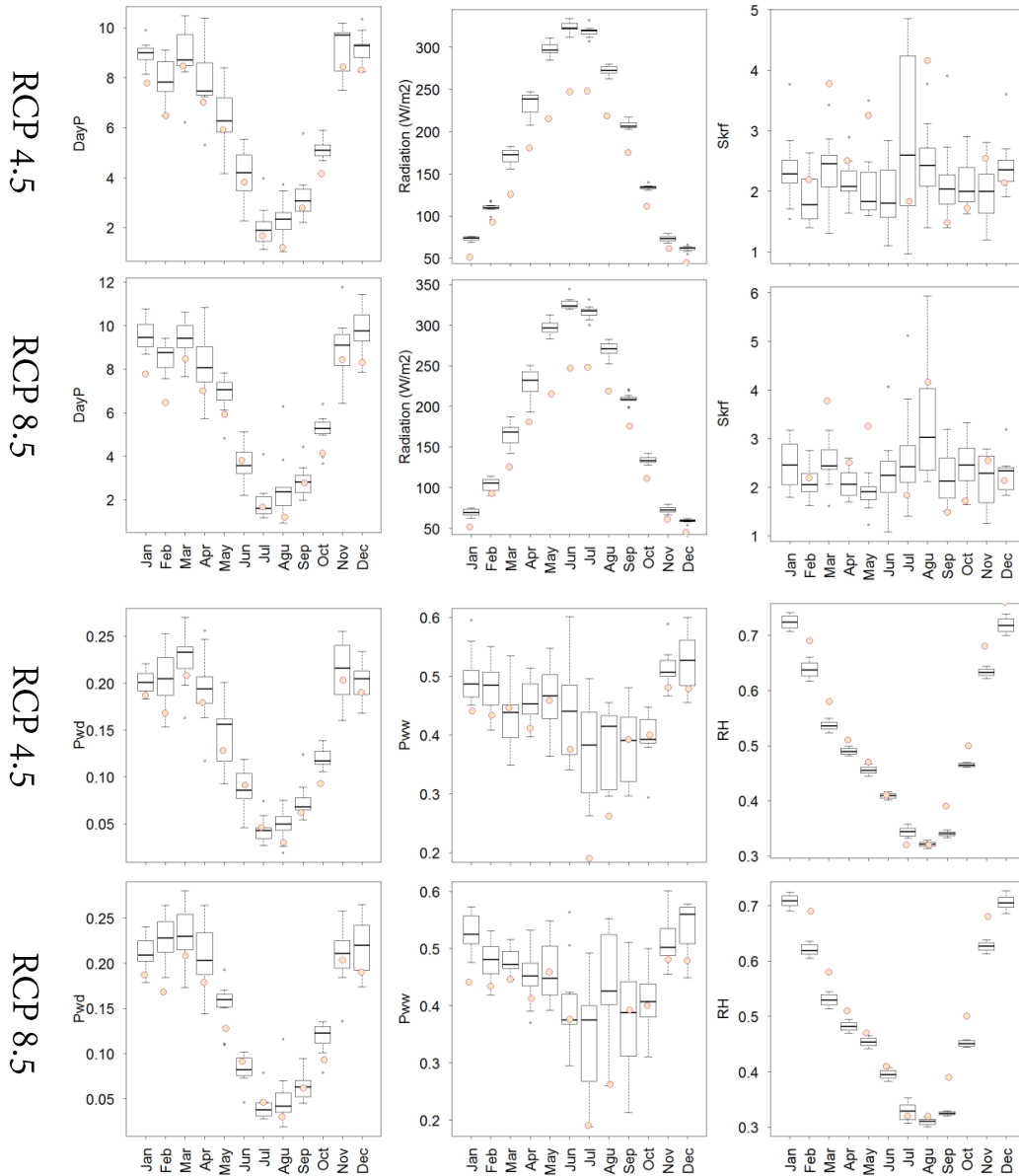


- 875 Qian, B., S. Gameda, H. Hayhoe, R. De Jong, and A. Bootsma (2004), Comparison of  
876 LARS-WG and AAFC-WG stochastic weather generators for diverse Canadian  
877 climates, *CLIMATE RESEARCH.*, 26(3), 175-191.
- 878 Richardson, C. W. (1981), Stochastic simulation of daily precipitation, temperature, and  
879 solar radiation, *Water Resources Research*, 17(1), 182-190.
- 880 Richardson, C. W., and D. A. Wright (1984), WGEN: A model for generating daily  
881 weather variables, edited, US Department of Agriculture, Agricultural Research  
882 Service Washington, DC, USA.
- 883 Semenov, M. A., and E. M. Barrow (1997). Use of a stochastic weather generator in the  
884 development of climate change scenarios. *Climatic change* 35.4: 397-414.
- 885 Stocker, T. F. (2014), Climate change 2013: the physical science basis: Working Group  
886 I contribution to the Fifth assessment report of the Intergovernmental Panel on  
887 Climate Change. *Cambridge University Press*. Cambridge, England
- 888 Tarlock, A.D., (2000). Prior appropriation: Rule, principle, or rhetoric. *N.D.L. Rev.*, 76,  
889 p.881.
- 890 Urban, S. M., and C. R. Petrich (1996), water budget for the Treasure Valley aquifer  
891 system, *Treasure Valley Hydrologic Project Research Report, Idaho Department*  
892 *of Water Resources, Boise, Idaho.*
- 893 Vano, J.A., B. Nijssen and D.P. Lettenmaier (2015). Seasonal hydrologic responses to  
894 climate change in the Pacific Northwest. *Water Resources Research*, 51(4),  
895 pp.1959-1976. DOI: 10.1002/2014WR015909
- 896 Wilby, R. L., and T. M. L. Wigley (1997), Downscaling general circulation model output:  
897 a review of methods and limitations.
- 898 Wilks, D. S (2010). Use of stochastic weathergenerators for precipitation  
899 downscaling. *Wiley Interdisciplinary Reviews: Climate Change* 1.6: 898-907.
- 900 Will, R. E., M. W. Stuart, Z. B. Chris, and C. H. Thomas. (2013) Increased vapor  
901 pressure deficit due to higher temperature leads to greater transpiration and  
902 faster mortality during drought for tree seedlings common to the forest–grassland  
903 ecotone. *New Phytologist* 200, no. 2: 366-374. DOI: 10.1111/nph.12321.
- 904 Xu, C.Y. (1999), From GCMs to river flow: a review of downscaling methods and  
905 hydrologic modelling approaches. *Progress in Physical Geography: Earth and*  
906 *Environment*. 23 (2): 229-249. <https://doi.org/10.1177/030913339902300204>.
- 907
- 908



909 Appendix A: *Boxplot of monthly climate statistics (12 variables) of 11 selected GCMs.*  
 910 *The circles indicate the historical monthly average.*

911  
 912  
 913  
 914  
 915





916

